Title	The formation of ordered bismuth nanowire arrays within mesoporous silica templates
Author(s)	Xu, Ju; Zhang, Wenhua; Morris, Michael A.; Holmes, Justin D.
Publication date	2007-02-24
Original citation	Xu, J., Zhang, W., Morris, M. A. and Holmes, J. D. (2007) 'The formation of ordered bismuth nanowire arrays within mesoporous silica templates', Materials Chemistry and Physics, 104(1), pp. 50-55. doi: 10.1016/j.matchemphys.2007.02.043
Type of publication	Article (peer-reviewed)
Link to publisher's version	http://www.sciencedirect.com/science/article/pii/S0254058407001411 http://dx.doi.org/10.1016/j.matchemphys.2007.02.043 Access to the full text of the published version may require a subscription.
Rights	
Item downloaded from	http://hdl.handle.net/10468/8144

University College Cork, Ireland
Coláiste na hOllscoile Corcaigh

The Formation of Ordered Bismuth Nanowire Arrays within Mesoporous Silica Templates

Ju Xu, Wenhua Zhang, Michael A. Morris and Justin D. Holmes*

Department of Chemistry, Materials Section and Supercritical Fluid Centre, University College Cork, Cork, Ireland.

Fax: + 353 21 (0)4274097; Tel: +353 (0)21 4903608; E-mail: j.holmes@ucc.ie

Abstract

Bismuth nanowire arrays have been synthesized within the pores of ordered mesoporous silica templates using a supercritical fluid (SCF) inclusion technique. The formation of nanowires within the mesopores was confirmed by powder X-ray diffraction (PXRD), N_2 adsorption experiments and transmission electron microscopy (TEM). The formation of the bismuth nanowire arrays occurred through the initial binding of the bismuth precursor to the inner walls of the mesoporous channels, forming bismuth crystal seeds, which subsequently developed into wire-like structures. By varying the concentration of the bismuth precursor in the SCF pahse, the loading of bismuth nanocrystals within the mesoporous channels can be controlled. The effect that temperature had on the formation of bismuth nanocrystals within the mesopores was also investigated. The highest loading of bismuth nanocrystals inside the mesopores was obtained at reaction temperatures near the critical point of toluene.

Keywords: Bismuth, nanowire arrays, mesoporous silica, template, supercritical fluid.

1. Introduction

There is currently great interest in the development of simple thermoelectric devices, with no moving parts, that are energy efficient and do not use greenhouse gases for cooling or heating.[1] The efficiency of a thermoelectric device depends on the thermoelectric figure of merit, *ZT*, of the material from which it is comprised. The figure of merit can be defined by the equation:

$$ZT = \frac{s^2 \sigma T}{\kappa}$$

Where *S* is the thermoelectric power (Seebeck coefficient), σ is the electrical conductivity, and κ is the thermal conductivity. Currently, the highest values of *ZT* that have been reported are for $Bi_{2(1-x)}Sb_{2x}Te_{3(1-y)}$ alloys, such as $Bi_{0.5}Sb_{1.5}Te_3$, with a *ZT* value of approximately 1.0 at 300 K. However, an improvement by at least a factor of 2 is required for thermoelectric devices to be competitive with common vapor-compression technology [2, 3] One approach for increasing the *ZT* value of materials is to reduce their dimensions, i.e. to form nanostructures such as quantum wells (2 D) or quantum wires (1 D). [3] Bismuth, which typically does not exhibit a high *ZT* factor as a bulk material is predicted to show enhanced thermoelectric performance ($Z_{1D}T$ > 1) when formed as nanowires less than 10 nm in diameter [4, 5]. Thus, the ability to control the diameter of bismuth nanowires is likely to lead to high performance materials for thermoelectric applications. However, owing to the relatively low-melting point of Bi (271.3 °C), the high temperature approaches which are widely used to synthesize highly crystalline semiconductor nanowires (Si, Ge, GaN etc.), such as laser ablation, plasma-arc and chemical vapor deposition synthesis are inappropriate for the synthesis of bismuth nanowires.[6] A low-temperature solvothermal process has recently been reported by many groups for synthesizing free-standing single crystalline bismuth nanowires and nanotubes [6-9]. Whilst this synthesis procedure is a significant break through in the production of Bi nanowires, the wires obtained are produced as tangled meshes which require further processing to separate them. Also, the diameters of the nanowires produced were between 20-30 nm which is well above the diameters required to obtain a high *ZT* value for Bi. One promising technique for the production of ordered arrays of bismuth nanowires is their incorporation into well-defined architectures. A number of groups have used anodized aluminium oxide (AAO) membranes as templates for forming bismuth nanowires using techniques such as electrochemical deposition [10, 11], vapor-phase techniques [12] and pressure injection processes [13]. Whilst the use of AAO membranes as templates has some application, it is difficult to obtain Bi nanowires which exhibit better thermoelectric properties than bulk state-of-the-art thermoelectric materials, as the pore diameter of the templates is typically larger than 10 nm.

Hexagonal mesoporous silica materials with uniform pore diameters, between 2-30 nm have been utilized as hosts to accommodate semiconductors [14-16], metals [17, 18] and metal oxide [19] nanowires and particles for many years. Nanoclusters can be deposited within the mesopores using techniques such as incipient wetness and ion exchange[16, 18, 20], surface modification methods [19, 21], metal–organic chemical vapor infiltration (CVI) and chemical vapour deposition (CVD).[22, 23] However, wet impregnation and ion exchange methods usually result in a low dispersion yield of the guest material within the mesopores because the precursors can easily diffuse onto the outer surface of the host silica.[24] Surface modification can prevent large particles forming on the outer surface of the host silica, but this method is only effectively applied to metal ions that can bind with silane coupling agents, such as some noble metal ions and soft acid metal ions, e.g. Zn^{2+}, Cd^{2+} etc. Besides, the loading is

limited by the amount of silane coupling agents bound to the surface Si-OH bonds.[25] Additionally, using liquid approaches it is often difficult to obtain a high yield of nanocrystals within the mesopores due to pore plugging; as the surface tension of the liquid solvent prevents precursor penetration into the pores. CVI and CVD approaches are less prone to pore plugging but can undergo capillary condensation resulting in liquid phase blocking of the pores. [26] Also, long deposition times are usually required to obtain a high loading of nanoclusters within the pores using these gas-phase inclusion methods.[24] Our laboratories have developed a number of supercritical fluid (SCF) solution-phase methods for forming metal, metal oxide and semiconductor nanowires within mesoporous materials with high loading levels, i.e. up to 90 %.[14, 15, 27-29] The high-diffusivity, low viscosity and reduced surface tension of a SCF leads to substantial solvent penetration of the porous matrix and rapid transport of the precursors into the mesopores where nucleation and growth of the nanowire arrays readily occurs, without pore blocking.[27]

In this paper, we describe an adaptation of a SCF inclusion technique to form ordered arrays of bismuth nanowires within mesoporous silica matrices. The effect that temperature has on the formation of bismuth nanowires within the mesoporous channels is discussed in detail. By controlling the reaction temperature around the critical point of toluene, the highest loading of bismuth inside the channels was obtained. In addition, the mechanism of bismuth formation within the mesopores is also described.

2. Experimental details

2.1 Syntheis of mesoporous silica

The synthesis of hexagonal mesoporous silica has been comprehensively described in previous work [30], *ie*. the hydrolysis of tetraethoxysilane (TEOS) in the presence of a poly(ethylene oxide)(PEO)-polypropylene oxide(PPO) triblock copolymer surfactant, Synperonic P85($PEO_{26}PPO_{39}PEO_{26}$) or P123($PEO_{20}PPO_{69}PEO_{20}$) and HCl (0.5 M). In a typical synthesis, Synperonic P85 (1.0 g) was dissolved in TEOS (1.8 g) and added to an aqueous solution of HCl (1.0 g, 0.5 M). Ethanol generated during the reaction was removed on a rotary evaporator at 40 ℃. The resulting viscous gel was left to condense at 40 ℃ for 1 week in a sealed flask. Calcination of the silica was undertaken in air for 24 hrs at 500 ℃. The silica matrices were degassed prior to inclusion using the Flow Prep 060 Degasser (Micrometrics). Pure, dry N_2 was passed over the heated mesoporous matrix at 200 ℃ to remove moisture.

2.2 Fabrication of Bi nanowire arrays

Bismuth nanowires were synthesized within the mesoporous silica powder by degrading triphenylbismuth in supercritical or near supercritical toluene solvents. In a typical procedure, mesoporous silica powders (0.1 g) and triphenylbismuth (0.5 – 4.1 mmol) were added to a high pressure reaction cell (~21 ml) inside a nitrogen glovebox. The reaction cell was attached, via a three-way valve, to a stainless steel high pressure tube (~50 ml) equipped with a stainless steel piston. An ISCO syringe pump (Lincoln, NE) was used to pump carbon dioxide into the back of the piston and displace oxygen-free anhydrous toluene solvent into the reaction cell to 34.5 MPa. The reaction cell was placed into a tube furnace and heated to the reaction temperature between 250 to 400 ℃ for about 2 - 12 hrs. After the reaction, the cooled product was washed by acetone prior to analysis.

2.3 Characterization

Transmission electron microscopy (TEM) was performed on a JEOL 2000FX operating at 200 KV. Powder X-ray diffraction (PXRD) data was collected on a Philips PW3710 MPD diffractometer using Cu K_{a1} radiation with an anode current of 40 mA and an accelerating voltage of 40 kV. A micrometrics Gemini III 2375 surface area analyzer was used to collect the Brunauer-Emmett-Teller (BET) surface area and Barrett, Joyner and Halenda(BJH) pore size distributions. Fourier transform infrared (FTIR) spectroscopy was measured on a Bio-Rad FTS 3000 FTIR spectrophotometer.

3. Result and Discussion

3.1 Bismuth nanowire formation

Figure 1 shows low angle PXRD patterns of calcined P85 mesoporous silica before and after bismuth inclusion. Three peaks can be indexed to the (100), (110) and (200) reflections for a hexagonal mesoporous solid consisting of well ordered channels. The position of the intense (100) peak reflects a d spacing of 7.2 nm corresponding to a pore-to-pore distance of 8.3 nm. Inclusion of bismuth into the mesopores results in the gradual decrease in intensity of the (100) peak and loss of the (110) and (200) diffraction peaks as we have previously observed for the inclusion of silicon into silica mesopores.[14, 15] This loss in intensity, which results from increased residual strain on the silica walls upon inclusion,[31] increases as a function of precursor concentration and is a good indication that the mesopores are being filled with bismuth.[15, 16]

The purity and crystallinity of the bismuth nanowires were confirmed by PXRD at high angles (figure 2). The sharp peaks in the PXRD pattern can be indexed to a rhombohedral structure with a lattice constant a = 4.5288 Å, c = 11.7660 Å which is in good agreement with the reported PXRD data (JCPDS card No. 851329) and a lattice constant a = 4.5460 Å, c = 11.8620 Å.

Figure 3 shows the infra-red spectra of calcined mesoporous silica before and after bismuth inclusion. The silanol vibrational modes, an O-H stretch (v_s(O-H)) at 3700-3200cm^{-1} and Si-O bending mode (v_B(Si-O)) at 955-835 cm^{-1}, are present in the mesoporous silica sample before bismuth inclusion. After the formation of bismuth nanowires, the intensity of the O-H stretching mode is greatly reduced,

suggesting the anchoring of bismuth nanowires to the mesoporous walls[32].

Figures 4 a and b display the nitrogen sorption isotherms and the BJH pore size distributions of calcined P85 mesoporous silica before and after inclusion of bismuth nanowires. For comparison, the sorption isotherms and the pore size distributions of mixtures of mesoporous silica and bismuth powders are shown in figure 4(c) and (d). All samples exhibit well-defined hysteresis loops of type H1, according to the IUPAC classification,[33] associated with capillary condensation and desorption in open-ended cylindrical mesopores. The isotherms for the bismuth-loaded mesoporous samples are similar in shape to the as-synthesised calcined mesoporous silica sample, suggesting that preservation of the host structure remains after bismuth inclusion.[19] For the bismuth-loaded mesoporous samples, the surface area and the pore volume decrease, the hysteresis loops shift to a smaller relative pressure and the mean pore diameter decreases with increasing precursor concentration. However, for the samples of mixed mesoporous silica and bismuth powders, in which there is no bismuth inside the channels of the silica, no shift in the hysteresis loops and no change in the mesopore diameters were observed with increasing bismuth concentration; although the surface area and the adsorbed volume do decrease due to the dilution of the parent mesoporous silica by bismuth[34]. These results confirmed that in our SCF preparation, bismuth can be incorporated inside the silica mesopore channels using triphenylbismuth as a precursor. Moreover, these results also indicate that if the loading of bismuth inside the channels was calculated simply based on the reduction of pore volume,[14] the calculated loading would not reflect the true amount of bismuth inside the mesopores. Therefore, the loading of bismuth inside the channels was subsequently calculated by the reduction in the mesopore diameter. Table 1 shows how the loading of bismuth inside the mesoporous channels increases with increasing bismuth precursor concentration, indicated by a decrease in the mean pore diameter. By varying the concentration of the Bi precursor in the SCF, the loading of bismuth nanocrystals inside the mesoporous channels can be controlled,up to a loading of 33 %.

Figure 5 shows TEM images of hexagonal mesoporous silica before and after bismuth nanowire inclusion. The bismuth nanowires appear as dark continuous rod-like objects inside the host matrix following the direction of the nanoscale channels. EDX analysis carried out on the Bi-mesoporous silica samples shows strong Bi and Si signals. The Bi nanowires formed within the mesoporous channels have uniform diameters, consistent with the pore diameters of the parent mesoporous silicas, i.e. P85 and P123 templated mesoporous silicas give 5 and 8 nm Bi nanocrystals respectively, (see figure 5 a to e). The view perpendicular to the pores (figure 5 e) clearly reveals the hexagonal ordering of the Bi-filled mesopores, suggesting that the mesopores contain bismuth nanowires. Free-standing bismuth nanowires after removal of the silica matrix, by a 6 M NaOH solution, is shown in figure 5 f. The average diameters of those free standing nanowires are around 5.0 nm, which is consistent with the mean diameter of the mesoporous channels from which they were removed. Even after removal of the silica template, the Bi nanowires appear to still be linked together in arrays, i.e adjacent nanowires are aligned side-by-side and the relative positions of adjacent nanowires are largely the same as in the mesoporous template, probably due to interconnecting micropores between the nanowires[35]. A SAED pattern of isolated Bi nanowire arrays (Figure 5(f) inset) gives a ring pattern that can be indexed to the (012), (110) and (024) planes of rhombohedral Bi, confirming the multi-crystalline structure of the Bi nanowires. In addition, many vacant pores, a well-known phenomena for mesoprous nanocomposites,[16, 20] were also observed, indicating that only a portion of mesopores can be filled. This may be explained by understanding the mechanism by which the bismuth nanowires are formed. In our method, the nanowires are formed within the silica mesopores through the initial binding of the precursor with the active silanol groups on the inner walls to form bismuth crystal seeds. These seeds subsequently grow to form wire-like structure (not tube-like structure as our Si,Ge and Co inclusion[15, 27, 36], probably due to the low melting point, 270 ºC, of bismuth and poor wettability of liquid bismuth with the silica walls [37]) within the channels with increasing metal atom deposition. However, silanol groups also exist on the external surface of the silica and some bismuth crystal seeds may also be formed on these sites, and grow into particles without limitation. At the beginning of the reaction, the high-diffusivity of the SCF and the larger number of silanol groups inside the mesopores compared to the outside surface may result in more bismuth forming inside the mesopores than outside. As the reaction proceeds, bismuth starts to fill the pores, making it harder for the bismuth precursor to diffuse into the mesoporous channels. Hence, the precursors may then readily decompose on the outer surfaces, resulting in uncompletely bismuth filling inside the mesopores.

3.2 The effect of reaction temperature

In our experiments, using toluene as the SCF, the pyrolysis of triphenylbismuth to form crystalline bismuth nanowires was found to be temperature dependent. Pyrolysis of triphenylbismuth was observed at temperatures above 250 ºC and the rate of decomposition was found to increase with increasing temperature. The decomposition rate at 250 ºC was slow, even after 12 hours the precursor was not fully decomposed, compared to temperatures of 270 ºC and 320 ºC where decomposition of the precursor was completed after 12 and 2 hours respectively. Figure 6 displays the nitrogen sorption isotherms and the BJH pore size distribution of as-calcinated P85 templated mesoporous silica reacted with triphenylbismuth at different temperatures. Compared to the parent mesoporous silica, the shift in the hysteresis loop to smaller relative pressure and the decrease in the mean pore diameter at 320 ºC are the most obvious changes, suggesting the highest loading of bismuth was obtained at this

3

temperature. This temperature dependence can be explained by considering the crystal growth. [38] The effective growth of bismuth nanowires inside the channels of mesoporous silica occurs through the heterogeneous nucleation and growth of bismuth crystals on the inner pore walls, which depends on the rate at which the precursor is transported into the pores and the rate at which the precursor decomposes. SCFs are an ideal media for the rapid and effective transport of material into porous structures due to their low viscosity and negligible surface tension[39]. Unlike gas phase techniques, such as CVD, SCFs can not be condensed to liquids inside the mesoporous channels resulting in pore blocking. In our experiments, as outlined in figure 6, if the reaction temperature is too high, above 400 ℃, no reduction in the pore diameter was observed, indicating most of bismuth formed outside the mesoporous channels as bismuth particles. Under these conditions the rate of decomposition of triphenylbismuth is so fast that nucleation and growth occurs before the precursor can reach the inner surface of the mesoporous walls. Hence, in our experiments, a lower loading of bismuth was observed at the temperature of 400 ℃ compared to 320 ℃. If the reaction temperature is too low, *i.e.* 270 ℃, which is below the critical point of toluene (Tc=319 ℃, Pc=4.1 MPa), the lower diffusion rate of the toluene as a high pressure liquid, compare to its SCF state, results in significant amounts of bismuth forming on the outside of the mesoporous channels. Therefore, a lower loading of bismuth was found inside the channels at a temperature of 270 ℃ compared to 320 ℃.

Thus, to achieve a high loading of bismuth nanowires inside the channels mesoporous silica, controlling the diffusion rate and the decomposition rate of the precursor is important. In our experiments, the highest loading of bismuth nanowires inside the channels of mesoporous silica was obtained when the reaction temperature was close to the critical point of toluene, i.e. 320 ℃.

4. Conclusions

Nanowires of bismuth have been successfully prepared within the channels of mesoporous silica through the decomposition of the diphenylbismuth under SCF condition. The amount of bismuth loaded inside the mesopores can be controlled by varying the precursor concentration. The highest loading of bismuth inside the channels of the mesoporous silica was obtained when the reaction temperature was controlled close to the critical point of toluene.

Acknowledgements

References

[1] B. C. SALES, *Science* **2002**, *295*, 1248.

[2] D. M. ROWE, *Handbook of thermoelectrics*, Chemical Rubber Company, Florida, **1995**.

[3] T. TRITT, *Recent trends in thermoelectric materials research III semiconductors and semimetalss 71: IX-XIV*, Academic Press INC. San Diego IDS, **2001**.

[4] L. D. HICKS, M. S. DRESSELHAUS, *Phys. Rev. B* **1993**, *47*, 16631.

[5] X. SUN, Z. ZHANG, M. S. DRESSELHAUS, *Appl. Phys. Lett.* **1999**, *74*, 4005.

[6] Y. GAO, H. NIU, C. ZENG, Q. CHEN, *Chem. Phys. Lett.* **2003**, *367*, 141.

[7] Y. LI, J. WANG, Z. DENG, Y. WU, X. SUN, D. YU, P. YANG, *J. Am. Chem. Soc.* **2001**, *123*, 9904.

[8] X. LIU, J. ZENG, S. ZHANG, R. ZHENG, X. LIU, Y. QIAN, *Chem. Phys. Lett.* **2003**, *374*, 348.

[9] H. YU, C. PATRICK, G. WILLIAM, E. BUHRO, *J. Mater. Chem.* **2004**, *14*, 595.

[10] Y. PENG, D. QIN, R. ZHOU, H. LI, *Mater. Sci. Eng. B - Solid Stat Mater. For Adv. Tech.* **2000**, *77*, 246.

[11] C. JIN, G. JIANG, L. WF, W. CAI, L. YAO, Z. YAO, X. LI, *J. Mater. Chem.* **2003**, *13*, 1743.

[12] J. HEREMANS, C. THRUSH, Y. LIN, S. CRONIN, Z. ZHANG, M. DRESSELHAUS, J. MANSFIELD, *Phys. Rev. B* **2000**, *61*, 2921.

[13] Z. ZHANG, D. GEKHTMAN, M. DRESSELHAUS, J. YING, *Chem. Mater.* **1999**, *11*, 1659.

[14] N. COLEMAN, N. O'SULLIVAN, K. RYAN, T. CROWLEY, M. MORRIS, T. SPALDING, D. STEYTLER, J. HOLMES, *J. AM. Chem. Soc.* **2001**, *123*, 7010.

[15] N. COLEMAN, M. MORRIS, T. SPALDING, J. HOLMES, *J. Am. Chem. Soc.* **2001**, *123*, 187.

[16] F. BRIELER, P. GRUNDMANN, M. FROBA, L. CHEN, P. KLAR, W. HEIMBRODT, H. V. NIDDA, T. KURZ, A. LOIDL, *J. Am. Chem. Soc.* **2004**, *126*, 797.

[17] W. ZHOU, J. M. THOMAS, D. S. SHERHARD, B. F. G. JOHNSON, D. OZKAYA, T. MASCHMEYER, R. G. BELL, Q. GE, *Science* **1998**, *280*, 705.

[18] G. KHITROV, *MRS Bull.* **2000**, *25*, 6.

[19] W. ZHANG, J. SHI, L. WANG, D. YAN, *Chem. Mater.* **2000**, *12*, 1408.

[20] M. H. HUANG, A. CHOUDREY, P. D. YANG, *Chem. Commun.* **2000**, 1063.

[21] W. ZHANG, J. SHI, H. CHEN, Z. HUA, D. YAN, *Chem. Mater.* **2001**, *13*, 648.

[22] H. KANG, Y. JUN, J. PARK, K. B. LEE, J. CHEON, *Chem. Mater.* **2000**, *12*, 3530.

[23] K. B. LEE, S. M. LEE, J. CHEON, *Adv. Mater.* **2001**, *13*, 517.

[24] J. SHI, Z. HUA, L. ZHANG, *J. Mater. Chem.* **2004**, *14*, 795.

[25] F. GAO, Q. LU, X. LIU, Y. YAN, D. ZHAO, *Nano Lett.* **2001**, *1*, 743.

[26] K. J. ZIEGLER, B. POLYAKOV, J. S. KULKARNI, T. A. CROWLEY, K. M. RYAN, M. A. MORRIS, D. ERTS, J. D. HOLMES, *J. Mater. Chem.* **2004**, 585.

[27] T. CROWLEY, K. ZIEGLER, D. LYONS, D. ERTS, H. OLIN, M. MORRIS, J. HOLMES, *Chem. Mater.* **2003**, *15*, 3518.

[28] K. ZIEGLER, P. HARRINGTON, K. RYAN, T. CROWLEY, J. HOLMES, M. MORRIS, *J. Phys. Cond. Matt.* **2003**, *15*, 8303.

[29] SING K.S.W. , EVERETT D.H., HAUL R.A.W., MOSCOU L., PIEROTTI R. A., ROUQUEROL J., S. T., *Pure Appl. Chem.* **1985**, *57*, 603-619.

[30] K. RYAN, N. COLEMAN, D. LYONS, J. HANRAHAN, T. SPALDING, M. MORRIS, D. STEYTLER, R. HEENAN, J. HOLMES, *Langmuir* **2002**, *18*, 4996.

[31] MARLER B, OBERHAGEMANN U, VORTMANN S, G. H, *Microporous Mater.* **1996**, *6*, 375.

[32] X. S. ZHAO, G. Q. LU, A. K. WHITTAKER, G. J. MILLAR, H. Y. ZHU, *J. Phys. Chem. B* **1997**, *101*, 6525-6531.

[33] S. J. GREGG, K. S. W. SING, *Adsorption Surface Area and Porosity*, Academic Press, New York, **1982**.

[34] L. VRADMAN, M. V. LANDAU, D. KANTOROVICH, Y. KOLTYPIN, A. GEDANKEN, *Microporous Mesoporous Mater.* **2005**, *79*, 307-318.

[35] R. RYOO, C. H. KO, M. KRUK, V. ANTOCHSHUK, M. JARONIEC, *J. Phys. Chem. B* **2000**, *104*, 11465-11471.

[36] J. D. HOLMES, D. M. LYONS, K. J. ZIEGLER, *Chem. Eur. J.* **2003**, *9*, 2144.

[37] Z. ZHANG, Massachusetts institute of technology **1999**.

[38] P. HARTMAN, in *North-Holland Series in Crystal Growth 1* (Eds.: W. BARDSLEY, D. T. J. HURLE, J. B. MULLIN), North-horland Pulishing Company, Amsterdam, **1973**.

[39] T. CLIFFORD, *Fundamental of Supercritical Fluids*, Oxford University Press, Oxford, **1998**.
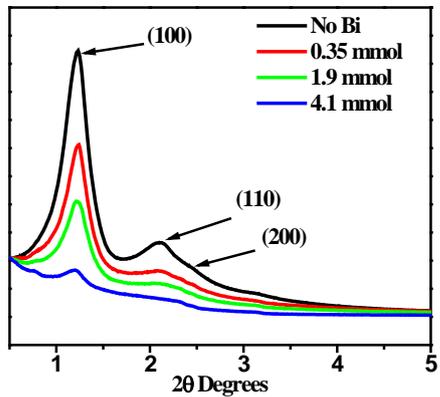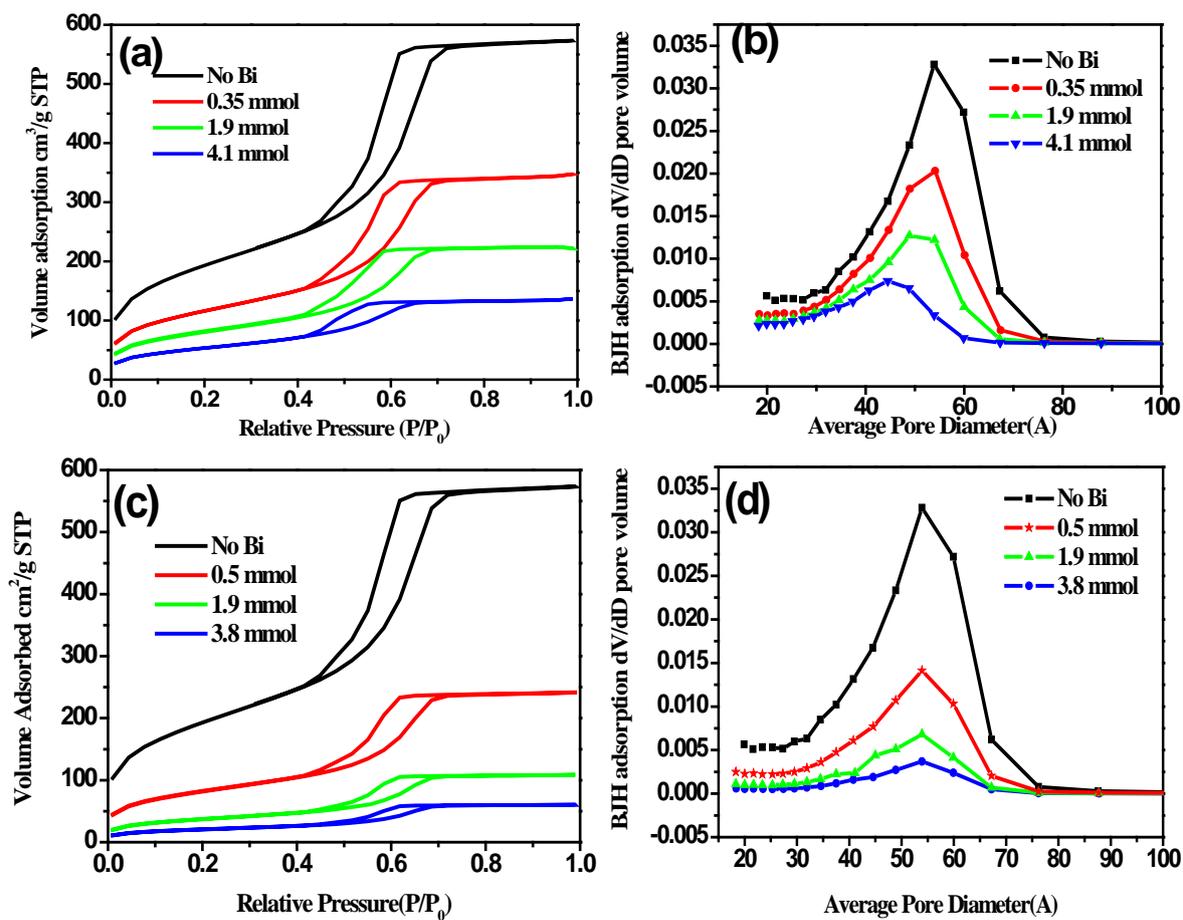
Figure 1 Low angle PXRD patterns of as-synthesized P85 mesoporous silica before and after bismuth inclusion formed by degrading triphenylbismuth at 320 ºC for 2 hours. PXRD patterns for bismuth concentration of 0.35, 1.9 and 4.1mmol, relative to 0.1 g of mesoporous silica, are shown.
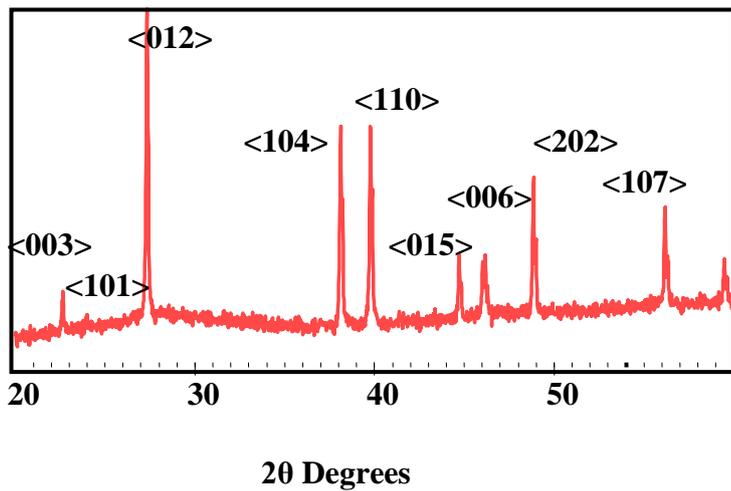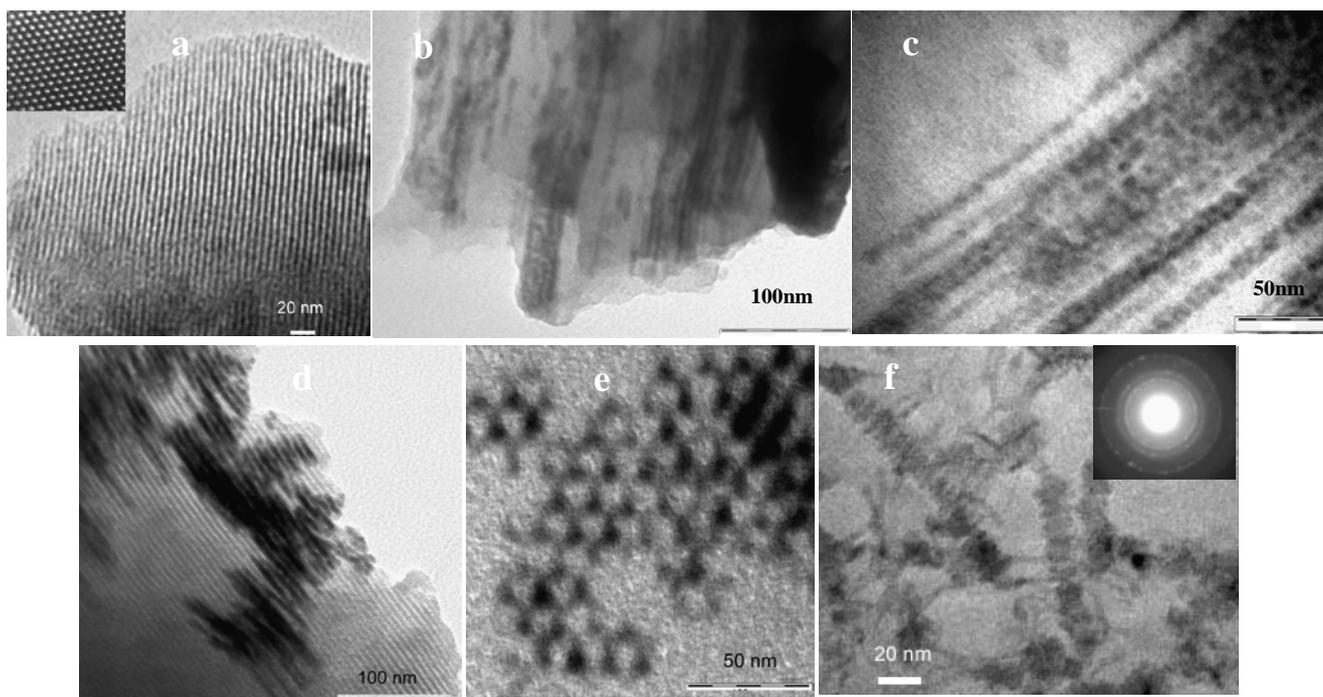
Figure 2 High angle PXRD pattern of Bi-filled P85 mesoporous silica formed by degrading triphenylbismuth at 320 ℃ for 2 hours
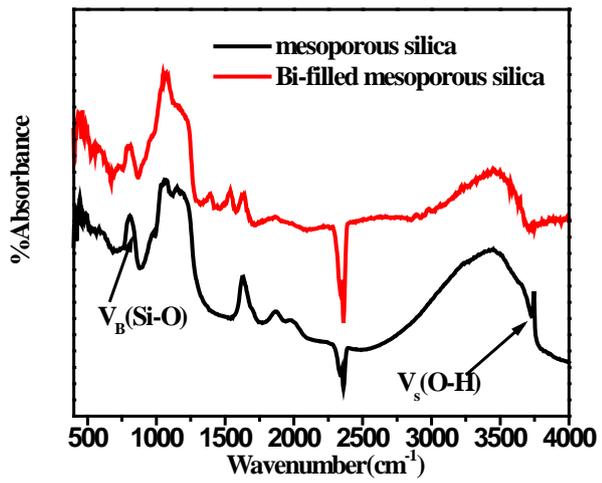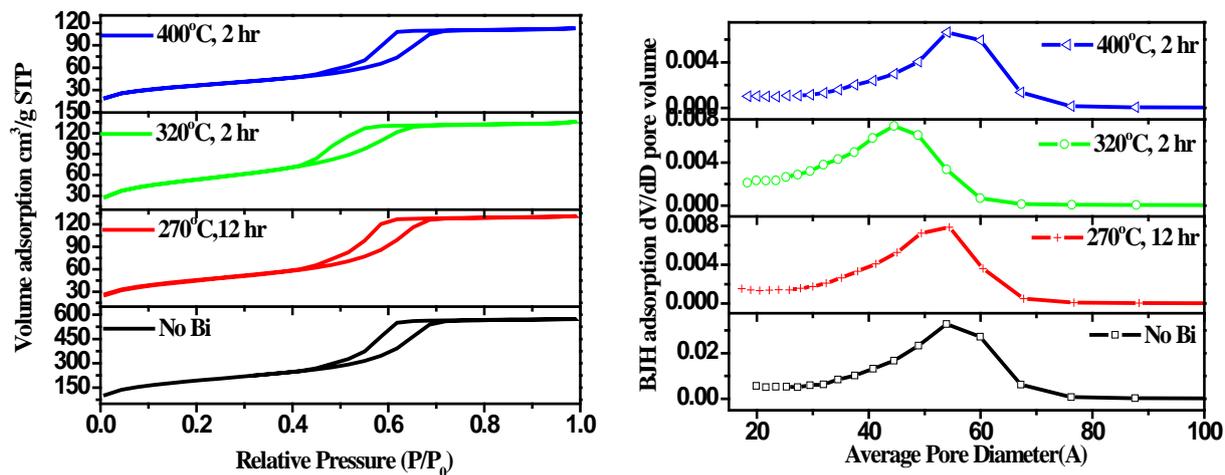
Figure 3 FTIR spectra of P85 mesoporous silica before and after bismuth inclusion

Figure 4 Nitrogen sorption isotherms (a) and Pore-size distributions (b) of as-synthesized P85 mesoporous silica before and after bismuth inclusion at 320°C; Nitrogen sorption isotherms (c) and Pore-size distributions (d) of as-synthesized P85 mesoporous silica and the mechanical mixtures of bismuth and mesoporous silica powders.

Figure 5 TEM images of a) as-synthesis P85 mesoporous silica, b,c) Bi-filled P85 mesoporous silica, d,e) Bi-filled P123 mesoporouse silica, f) free-standing bismuth after removing the P123 silica matrices, all Bi filled mesoporous silica samples were formed by degrading triphenylbismuth at 320 ºC for 2 hours.

Figure 6 Nitrogen sorption isotherms and the pore-size distribution of as-synthesized mesoporous silica and Bi-filled P85 mesoporous silica at different temperatures.

Table 1 Parameters of the as-synthesised P85 mesoporous silica before and after bismuth inclusion

Precursor concentration m_i (mmol)	Theoretical loading [a] R_t (%)	Surface area A_i (m^2/g)	Adsorbed volume V_i (cm^3/g)	Mean pore diameter D_i (Å)	Bi loading inside the channels [b] R (%)
0	0	691.5	0.81	55	0
0.35	9%	418.0	0.50	54	4%
1.9	50%	289.9	0.32	50	17%
4.1	108%	194.0	0.19	45	33%

[a] The theoretical loading is calculated by: $R_t = \dfrac{m_i M_{Bi}}{d_{Bi}} \times \dfrac{1}{V_0} \times 100\%$

(M_{Bi}: bismuth molecular weight, d_{Bi}: density of bismuth)

[b] The bismuth loading inside the channels is calculated by: $R = \dfrac{D_0{}^2 - D_i{}^2}{D_0{}^2} \times 100\%$